

3D MODELING OF STRUCTURES USING BREAK-LINES AND CORNERS IN 3D POINT CLOUD DATA

Hiroshi YOKOYAMA ^a, Hirofumi CHIKATSU ^a

^a Tokyo Denki Univ., Dept. of Civil Eng., Hatoyama, Saitama, 350-0394 JAPAN - yokoyama@chikatsu-lab.g.dendai.ac.jp, chikatsu@g.dendai.ac.jp

Commission V, WG V/4

KEY WORDS: Cultural Heritage, Modeling, Visualization, Laser scanning, Representation, Three-dimensional, Digital

ABSTRACT:

Recently, a laser scanner has been receiving more attention as a useful tool for real-time 3D data acquisition, and various applications such as city modeling, DTM generation and 3D modeling of cultural heritage were proposed.

However, 3D Representation of historical structures from point cloud 3D data collected by laser scanner is still issues. In order to reduce the time, labor and skill for archival recording of the cultural heritage, the authors discuss measuring system using 3D scanner and 3D modeling.

This paper describes on 3D representation of historical structure using laser scanner, effectiveness of 3D modeling using break-line.

1. INTRODUCTION

With respect to recording work, it is essential to reduce the amount of time, labor, and skill employed while making archival records of a historical structure. In order to do so a laser scanner is used to measure the sites, and on the basis of the results, an image of the model is constructed.

The Triangulated Irregular Network (TIN) model is generally generated for 3D modeling using all the measured points (HUAN, 1989), however, the large amount of point cloud data obtained by the laser scanner pose a problem.

Although the Marching Cube Algorithm (Laursen, Cline, 1987) is generated for reduction of the data values or the polygon number, the precision setting of the model changes.

This issue becomes a particularly serious problem in accurate 3D modeling. In this paper, the 3D modeling of a historical structure using a laser scanner and effectiveness of 3D modeling using break-line will be introduced.

2. 3D REPRESENTATION

Figure 1 shows workflow of certain processes for the 3D representation of the historical structure.

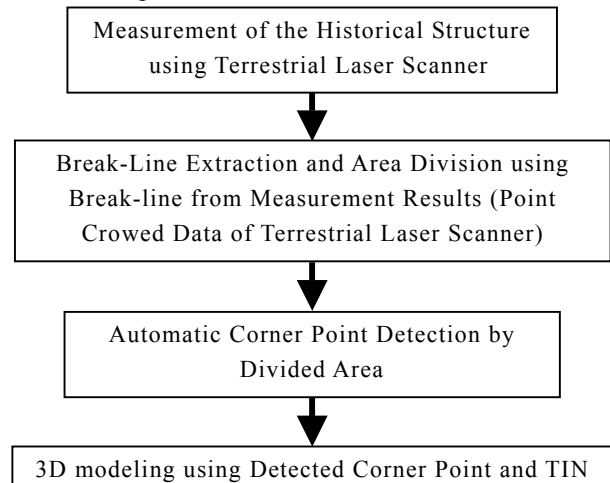


Fig.1 Flowchart for 3D Representation

Recently, the laser scanner has attracted considerable attention as measurement tool that can perform extensive 3D measurements in real time. A Total Station is used for this purpose in same purpose, but it requires a greater amount of labor and skill. So, the authors measured the historical structure and carried out 3D modeling

using laser scanners for labor saving. About modeling method, efficient corner detection method for 3D point cloud data was introduced. Though, effectiveness and accuracy were not described. This paper describes about effectiveness and accuracy of 3D modeling method by efficient corner detector for 3D point cloud data.

3. BREAK-LINE EXTRACTION

3.1 Outline of Modeling Process

The historical structure consists of several flat parts. Therefore, 3D modeling is enabled by the unification of all flat parts of historical structure. The break-lines provide the object edges and ridgelines, and these can be used to accurately determine the points to be modeled of the TIN model along with the flatness classification results. The technical outlines are presented later.

3.2 Classification of Flat and Non-Flat Areas

Break-lines are included in boundary of flat and non-flat part. Therefore, Classification of the flat and non-flat area is necessary before break-line extraction.

In order to classify flat and non-flat area, 3D point cloud data was acquired using terrestrial laser scanner. A small mask with 30*30 cm area is used instead of the 3D information samples. After a 3*3 point mask is generated around an interest point, the mask size expands to 30*30 cm by computing the plane coordinates for the neighbor points. The mask is then transformed so that in the first step, a normal vector for the mask becomes parallel to the Z-axis (Figure 2).

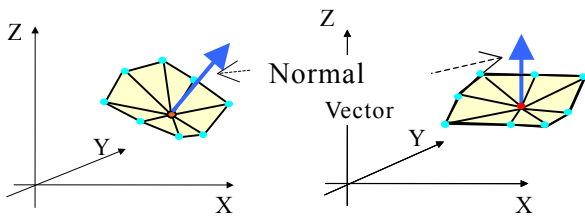


Fig.2 Coordinate Transformation

In the next step, the standard deviation (S.D.) is computed for the interest point. The threshold value should be considered while classifying the interest points into flat (ground surface, structure walls, etc.) and non-flat areas (trees, bushes, sky, etc.). The threshold value is

determined on the basis of the measured data, and it is set as 0.015m(=Rough Unpaved Road) in this paper.

3.3 Derivation of the Break-Lines

The break-lines (e.g., object edges, ridge-lines) provide important morphological information. Although these are indispensable features for DTM generation, city and object modeling, problems with automatic detection of the break-lines still persist. A technique for automatic detection of the break-lines using the flatness values was developed (H.YOKOYAMA, H. CHIKATSU,2004). The algorithm is closely related to edge-preserving smoothing, however, only the flat area is smoothed, and points with a larger S.D. within the non-flat area are emphasized. A small mask was used for smoothing. A mask size of 30*30 cm was sufficient, and an interest point was smoothed using the following equation:

$$g_j = \frac{\sum p_i \cdot \Delta g_{i,j}}{\sum p_i} \quad (1)$$

where,

g_j : S.D. for an interest point,

$\Delta g_{i,j}$: Difference in S.D. between an interest point and its neighboring points, defined as $\Delta g_{i,j} = g_i - g_j$,

p_i : Weight of the i point; where the weight is defined as the square of the values between the interest point and each neighboring point.

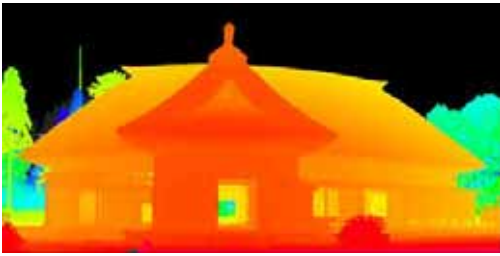
In order to detect the break-lines, smoothing of only the flat areas is repeated. By repeating process, the points with a larger standard deviation within the non-flat areas were emphasized. The break-lines were derived, and Figure 3 shows detected break-line for historical structure. Precise break line that was necessary for modeling were confirmed by comparing with manual detected break lines.

Figure 4 shows inspection method of break line extraction ability. In this paper, the target was measured at the same distance of historical structure (About 10m), and break line detection were done with changing thickness of targets (Thickness Range:0mm-100mm, 5mm pitch). As a result, break-line was extracted that the target had thickness more than 40mm. Figure 5 shows Detected Break-line(Thickness: 40mm).

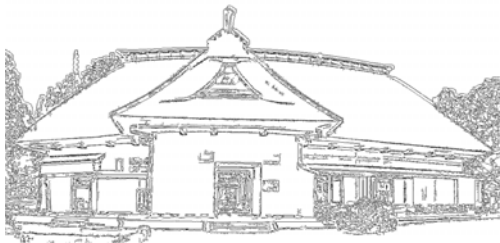
From these results, the aim that could apply proposal technique was confirmed.



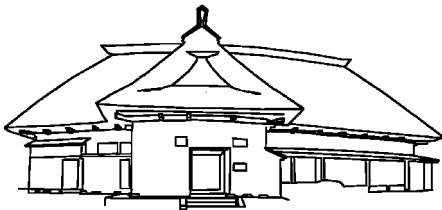
(a) Measurement Result (Intensity Data)



(b) Measurement Result (Range Data)



(c) Detected Break-lines (developed method)



(d) Detected Break lines (Manual)

Fig.3 Detection of The Break-Lines for Historical Structure

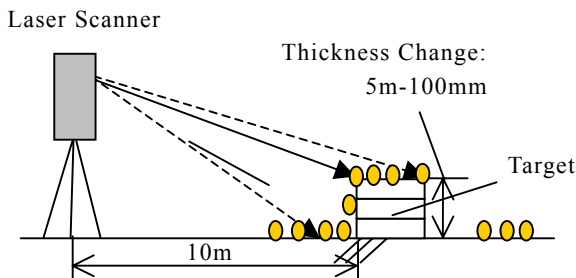
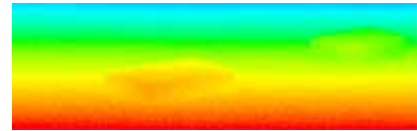


Fig.4 Inspection Method of Break-line Extraction Ability



(a) Range Image



(b) Detected Break-lines by developed method

Fig.5 Detected Break-lines

4. EFFICIENT CORNER DETECTOR METHOD

4.1 Extraction of the Corner Point

After the detection of break line, the shape of each area which was divided by break line will be obtained by tracing the outline of the area. When all curve points on the outline of the area are used to modeling, large number of data values are obtained. Therefore, the curve points that would be used to design the model detected by the following, and they were detected from the point cloud data to constitute the area.

"Curved point of the divided area by break line" is extracted using the principle of the inner product used in a vector. Figure 6 and the equation 2 shows the inner product.

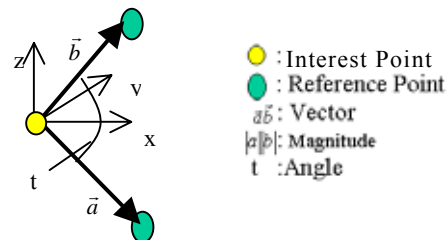


Fig.6 Conception of Inner Product

$$\vec{a}\vec{b} = |\vec{a}||\vec{b}|\cos t \quad (2)$$

where,

\vec{a}, \vec{b} = Vector,

$|\vec{a}|, |\vec{b}|$ = Magnitude (Distance of reference point and Interest point),

t = Angle

$$\vec{a}\vec{b} = (X_i - X_a)(X_b - X_i) + (Y_i - Y_a)(Y_b - Y_i) + (Z_i - Z_a)(Z_b - Z_i)$$

(X_i, Y_i, Z_i) = Position data of interest point,

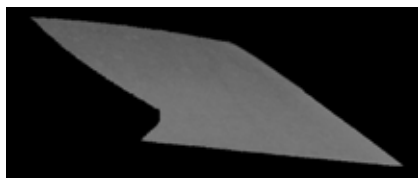
(X_a, Y_a, Z_a) = Position data of reference point

Figure 7 shows the angle data of sample flat area. This sample area is taken out by manual as a flat part of historical structure. The minimum angle in neighborhood of attention point becomes curved point. Therefore, there are many minimum angle points as curve point, and the curve point of the divided area can not extracted effectively.

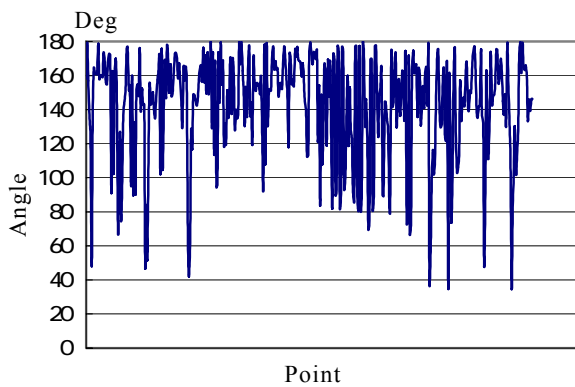
Many curve points are extracted from the flat area. Therefore, improvement of extraction method of curve point is demanded.



(a) Target Area (Intensity Image)



(b) Sample Flat Area (Intensity Image)



(c) Angle Data

Fig.7 Angle Data of Sample Flat Area

4.2 Evaluation of Projection Point

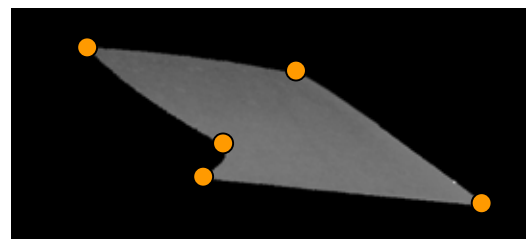
Historical Structure's roof is consists by stems of plant. In classification of the flat and non-flat areas, coordinate transformation using normal vector is done. A projection point is out from flat area after coordinate transformation, though, the point is classified as flat area by surroundings. When this situation was considered, the projection point removal will be performed by attention point removal that is not

included in flat area.

Figure 9(b) shows angle data without the projection points, and characteristic point as curve point can be confirmed by this result. But, fine changes which consist of influence of error are included in this data, yet.

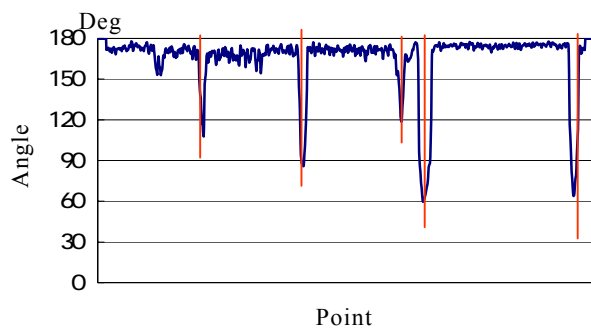
To detect only characteristic points automatically, only the characteristic points that space angles suddenly decrease should be extracted efficiently.

For automatic detection of characteristic points, authors notices that open changing likes resembled a two-dimensional signal wave pattern, and low level passage filter which can remove small wave pattern and detect big wave pattern from two-dimensional signal wave was used.



(a) Curve Point (Manually Detect)

on Intensity Image



(b) Angle Data without Projection Point

Fig.9 Angle Calculation Result after Projection

Point Removal

Sampling point number were limited on using a low level passage filter, FIR (limited reply analysis) filter which could make the low level passage filter which can set mask size was used in this paper.

Equation 3 shows definition function of an FIR filter, and parameter α for quantities of decrement are set for 7.857 which was determined by experience.

$$h_n = \begin{cases} \tilde{g}_n w_n, & |n| \leq L \\ 0, & |n| > L \end{cases} \quad (3)$$

Where,

h_n = Filter Coefficient, $2L+1$ =Filter Size

$$\tilde{g}_n = \begin{cases} g_n, & |n| \leq L \\ 0, & |n| > L \end{cases}, \quad g_n = \frac{1}{n\pi} \sin\left(\frac{2n\pi\omega_c}{\omega_s}\right),$$

$n = \dots, -1, 0, 1, 2, \dots$,

ω_c = interception angular frequency,

ω_s = specimen angular frequency

$$w_n = \begin{cases} \frac{I_0(\alpha\sqrt{1-(n/L)^2})}{I_0(\alpha)}, & |n| \leq L \\ 0, & |n| > L \end{cases},$$

$I_0(x)$ = first-class transformation Bessel function
of first

Figure 10(a) shows detected characteristic points by FIR filter. Removal of little change of angle data were confirmed from this result, and characteristic points are detected automatically by searching the smallest angle (peak value) from the data.

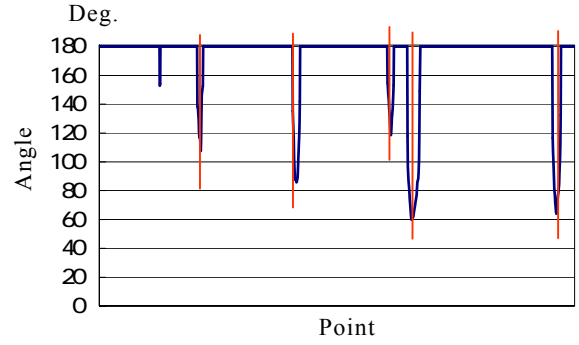
On the other hand, DOG (Difference of Gauss) function is applied to the new angle data, and the result which was calculated as 0 will be changed into 180 degrees as non-curve point. Equation 4 shows DOG function and figure 10(b) shows the detected characteristic points using DOG function.

$$DOG(x) = \int_{-\infty}^{\infty} \frac{1}{\sqrt{2\pi}\sigma_1} \exp\left(\frac{-x^2}{2\sigma_1^2}\right) * f(x) dx - \int_{-\infty}^{\infty} \frac{1}{\sqrt{2\pi}\sigma_2} \exp\left(\frac{-x^2}{2\sigma_2^2}\right) * f(x) dx \quad (4)$$

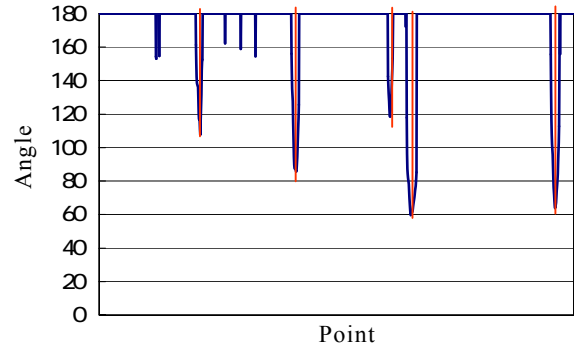
Where,

$DOG(x)$ = Result of DOG function, x = Distance from notice point to reference point,

$f(x)$ = Angle, σ_1 = Filter Size, $\sigma_2 = \sigma_1 * 1.6$



(a) FIR Filter



(b) DOG

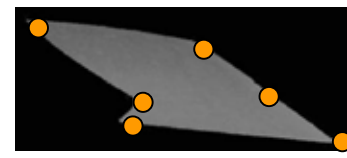
Fig.10 Detected Characteristic Points

In comparison with a result of FIR, result of DOG is including a lot of non-characteristic points. As a result, the effectiveness of presented method is confirmed.

5. 3D MODELING

5.1 TIN Model using Corner Points

TIN Model can make by using the detected characteristic points (curve points). By correspondence in the curve points and original image, textured model will be made. Figure 12 shows 3D model with a flat area. About the textured model making, camera calibration was done beforehand, and automatic correspondence is done with the result.



(a) Detected Curve Point



(b) TIN Model

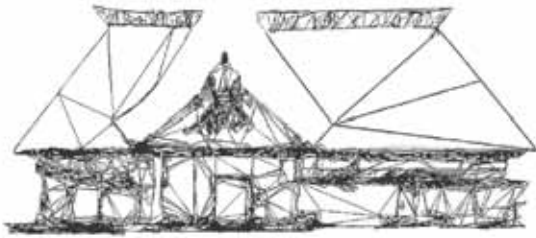
Fig.12 3D Model with a Flat Area

5.2 3D Modeling of Historical Structure

3D Modeling for the "Meguro residence" was investigated in this paper as one of applications using break-line. The Meguro residence was constructed in 1797 (about 200 years ago). Figure 13 shows 3D model obtained by measurement results.



(a) Original Image



(b) Wire Frame Model using a measurement result



(c) Textured Model using multiple measurement results (Front Image)



(d) Textured Model using multiple measurement results (Diagonal Course Image)

Fig.13 3D model using Obtained by Measurement Results

Table 3 shows comparison result about file size of 3D model as DXF file. MCA (Marching Cube Algorithm, Laurensen, Cline,1987) was proposed as 3D modeling method for extracting interesting parts in CT (Computer Tomography) and MR (Magnetic Resonance) image. By using present method, file size was greatly reduced in comparison with MCA.

Table3 Comparison result about file size

| Modeling Method | File Size |
|-----------------|-----------|
| Present Method | 1MB |
| MCA | 120MB |

6. CONCLUSION

The most remarkable points as results of this approach are its ability to file size of 3D modeling and accuracy at historical structure. As for further additional results of this investigation, utility of break-line to another targets can be archived. Therefore, we'll continue examination about automatic unification method of coordinate systems and effective modeling method.

REFERENCES

- 1.HUAN Y-P, 1989, Triangular irregular network generation and topographical modeling, Computer in industry, pp.203-213
- 2.W.E.Laurensen, H.E.Cline,1987, Marching Cubes: A High Resolution 3D Surface Construction Algorithm, Proc. ACM SIGGRAPH '87,ACM Press,pp.163-169
- 3.Brugelmann, R., 2000. Automatic breakline Detection from sairborne Laser Range Data. IAPRS, Vol.XXXIII, Part B3, Amsterdam, The Netherlands, pp. 109-116.
- 4.C.B.Jones, 1994, The implicit triangulated irregular network and multi-scale spatial databeses, Computer Journal, Vol.37,No.1, pp.43-57
- 5.H.YOKOYAMA, H. CHIKATSU,2004,Efficient Corner Detector for 3D point Crowd Data and application to 3D modeling of Structures,Proceedings of Electric Imaging Science and Technology "Videometrics VIII", Vol.5013, pp.208-215